Available online at www.sciencedirect.com
SCIENCE DIRECT
Icarus 182 (2006) 464–473
ICARUS
www.elsevier.com/locate/icarus

The magnetic field draping direction at Mars from April 1999 through August 2004

David A. Brain *, David L. Mitchell, Jasper S. Halekas

UC Berkeley Space Sciences Laboratory, 7 Gauss Way, Berkeley, CA 94720, USA

Received 12 April 2005; revised 19 September 2005

Available online 2 February 2006

Abstract

Using more than five years of data from the magnetometer and electron reflectometer (MAG/ER) on Mars Global Surveyor (MGS), we derive the draping direction of the magnetic field above a given latitude band in the northern hemisphere. The draping direction varies on timescales associated with the orbital period of Mars and with the solar rotation period. We find that there is a strongly preferred draping direction when Mars is in one solar wind sector, but the opposite direction is not preferred as strongly for the other solar wind sector. This asymmetry occurs at or below the magnetic pileup boundary (MPB), is observed preferentially on field lines that connect to the collisional ionosphere, and is independent of planetary longitude. The observations could be explained by a hemispherical asymmetry in the access of field lines to the low-altitude ionosphere, or possibly from global modification of the low-altitude solar wind interaction by crustal magnetic fields. We show that the draping direction affects both the penetration of sheath plasma to 400 km altitudes on the martian dayside and the radial component of the magnetic field on the planetary night side.

Keywords: Mars; Magnetic fields; Ionospheres; Solar wind

1. Introduction

The interaction of solar wind charged particles with a planet can be classified according to the type of obstacle that planet presents to the solar wind. Mars is unique in the solar system in this regard because its solar wind obstacle is a combination of its atmosphere and strong crustal magnetic fields (see Nagy et al., 2004, for a recent review). Like Venus, the atmospheric interaction appears to dominate the global solar wind interaction (Cloutier et al., 1999). Crustal fields significantly modify this interaction locally, and perhaps globally (Acuña et al., 2001; Mitchell et al., 2001; Brain et al., 2003; Crider, 2004; Brain et al., 2005). These fields rotate with Mars so that it continuously presents a different obstacle to the solar wind.

The solar wind carries the embedded interplanetary magnetic field (IMF), which propagates through the bow shock and drapes around the planetary obstacle. It has long been known that the orientation of the IMF will affect the global solar wind interaction with a planet (Dungey, 1961). At planets with large global magnetic fields, for example, IMF orientation determines whether magnetic reconnection is likely near the subsolar magnetopause (Paschmann et al., 1979). IMF direction also determines the direction of the solar wind convection electric field, $\vec{E}_{SW} = -\vec{v}_{SW} \times \vec{B}$, which in turn affects the motion of charged particles in the planetary interaction region. This effect is especially important for atmospheric obstacles, where a significant plasma population is in motion with respect to the solar wind.

At Mars, the IMF direction should influence the solar wind interaction in several ways. One main way is that planetary pickup ions are accelerated in the direction of $\vec{E}_{SW}$, so that ions are preferentially lost over one hemisphere (Cloutier et al., 1969). Another is that the direction of gyromotion of solar wind charged particles may affect the size, shape, and nature of plasma boundaries in the interaction region (Brecht and Ferrante, 1991). A third is that the IMF direction should affect magnetic field topology (the connectivity of magnetic field lines) near crustal sources, as magnetic reconnection of crustal

* Corresponding author. Fax: +1 (510) 643 8302.
E-mail address: brain@ssl.berkeley.edu (D.A. Brain).

0019-1035/$ – see front matter
doi:10.1016/j.icarus.2005.09.023

field lines to the IMF should be favored for some IMF orientations and not for others (Brain, 2002).

A number of IMF effects have been demonstrated using spacecraft observations. For example, the bow shock position is higher in the hemisphere toward which planetary pickup ions are accelerated (Zhang et al., 1991; Dubinin et al., 1998; Vignes et al., 2002). The MPB shape varies with the direction of draped magnetic fields near 400 km (Brain et al., 2005). Similarly, the magnetic field in the tail measured by the Phobos spacecraft is correlated with upstream IMF (Yeroshenko et al., 1990). The central tail has a plasma sheet containing oxygen streaming away from the planet that orients itself according to $\vec{E}_{SW}$ (Dubinin et al., 1991). And oxygen ions in the outer night side tail measured by the ASPERA instrument on Phobos were interpreted by Kallio et al. (1995) as escaping planetary pickup ions accelerated in the direction of $\vec{E}_{SW}$.

In this paper we report the results of a study of the draping direction of the magnetic field using more than five years of MGS MAG/ER observations from its circular mapping orbit. We outline our method for deriving draping direction in Section 2, and describe the three main effects in the data set (and their possible explanations) in Section 3. Then we use our derived draping directions to further explore its effect on two aspects of the global solar wind interaction at Mars: access of sheath plasma to 400 km altitudes on the day side, and the characteristic configuration of the magnetic field on the planetary night side. We summarize our results in Section 5.

2. Method

The MGS MAG/ER instrument and data set have been described in detail by Acuña et al. (2001). In this study we use data from the MGS mapping orbits from April 1999 through August 2004, recorded while the spacecraft was in a nearly circular orbit at 400 ± 30 km altitudes. The mapping orbit is fixed in local time at 2 pm, and the spacecraft orbital period is roughly two hours. MAG is a tri-axial fluxgate magnetometer that records full magnetic field vectors with a time resolution of 0.75, 1.5, or 3 s. The MAG instrument is physically located on the MGS solar panels rather than on a boom, so sophisticated calibrations are necessary to remove the contributions of magnetic fields from the spacecraft to observations. Calibrated MAG data are accurate to within 0.5 nT when MGS is in darkness, and 1 nT at other times (Acuña et al., 2001). Measured field magnitudes on the day side are typically on the order of 30–50 nT (Brain et al., 2003).

We are interested in how the direction of the upstream IMF affects the interaction of the solar wind with the martian atmosphere and crustal magnetic fields. However, there is no upstream solar wind monitor at Mars as there is for Earth. Therefore, we instead assume that the upstream IMF direction is directly related to the orientation of the draped magnetic field at the MGS mapping altitude. For each spacecraft orbit, we define an azimuth and elevation direction of the draped magnetic field based on all day side MAG data recorded between 50° and 60° North latitude, as illustrated in Fig. 1. Elevation direction is defined as the median angle that the measured field makes with the local horizontal. Azimuth direction is defined as the median direction of the horizontal field component, with 0° in the local eastward direction and 90° in the local northward direction.

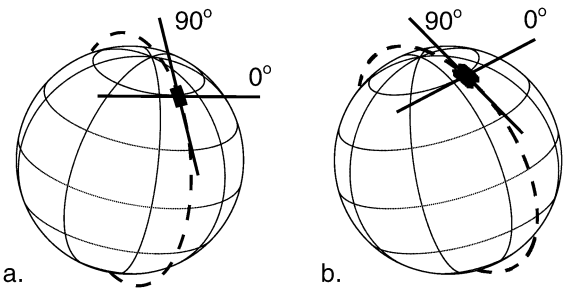

Fig. 1. MGS orbit geometry and definition of draping direction azimuth angle for (a) $L_S = 63°$ and (b) $L_S = 125°$. L_S is the solar longitude, and corresponds to martian season. The MGS orbit is shown as a dashed line. A rectangular box covers the portion of the orbit from 50°–60° North latitude. The horizontal components from MAG measurements in this region are used to derive the draping azimuth angle, which we define as 0° locally eastward and 90° locally northward. Elevation angle is defined with respect to the local horizontal.

In defining a field draping direction, we are constrained both by the fixed local time of the MGS orbit, and by the martian crustal magnetic fields. We have been careful to choose a latitude band lacking significant crustal magnetic fields in an effort to prevent internal fields from directly influencing our estimate of the external field orientation. However, as Fig. 1 shows, the intersection of this latitude band with the 2 pm orbit of MGS moves substantially with respect to the Sun over the course of a martian year, as the orientation of the planet's rotation axis with respect to the Sun changes. Finally, an estimate of the external field orientation for one portion of a spacecraft orbit in no way guarantees that the orientation is constant throughout the orbit. On the contrary, IMF direction changes on many time scales. Therefore, the analysis in Section 3 is confined to only those time periods when MGS was over the 50°–60° N latitude band. The analyses of Section 4 are statistical in nature, to minimize errors introduced from changes in draping orientation after the spacecraft leaves this latitude band.

We also use electron data to extract information about the plasma region and magnetic field topology that MGS experiences during our five year time period. The shape of an electron energy spectra recorded by ER indicates whether the spacecraft is in the martian sheath, pileup region, or ionosphere, as reported by Mitchell et al. (2001). Based on this idea, a method for identifying time periods when MGS was in or above the MPB was developed by Brain et al. (2005). In this study, the authors searched the MGS mapping data for a population of energized 100 eV electrons, which are created at the bow shock but lost to electron impact ionization or plasma depletion in the vicinity of the MPB (Crider et al., 2000; Øieroset et al., 2004). The presence of this population indicates that the spacecraft is between the bow shock and MPB.

Magnetic field topology is inferred primarily from the directional information of electrons recorded by ER in the form of pitch angle distributions (see Brain et al., 2004a, 2004b). Since we use electrons, we are only able to infer topology with respect to the absorption altitude for electrons in the martian

atmosphere. Open field lines (connected at one end to the atmosphere and the other to the draped IMF) have more electrons traveling toward Mars than away. Closed field lines (connected at both ends to the atmosphere) on the night side are either void of electrons or have fewer field-aligned electrons (a two-sided loss cone). On the day side, it is difficult to identify closed field lines from directional information because photoionization of the exosphere provides a continuous source of electrons with all pitch angles. Instead, we use the electron energy spectrum and search for the photoelectron features identified by Mitchell et al. (2001). Photoelectrons are readily apparent in ER observations only in the absence of electrons from the shocked solar wind—on closed field lines.

3. Distribution of draping direction

The derived draping direction for more than 22,000 MGS orbits from 1999 through August 2004 is shown in Fig. 2. Uncertainty in the determination of elevation angle was typically 3.1°, and was 5.5° for azimuth angle. Previous studies of MGS pre-mapping data (Brain et al., 2003; Crider et al., 2003) have demonstrated that the measured magnetic field on the martian day side is mostly horizontal. As the shocked solar wind interacts with the martian atmosphere, the embedded IMF drapes around the obstacle at the MPB (Bertucci et al., 2003). As expected, Fig. 2b shows that elevation angles cluster near 0°. However, the median elevation angle is negative (−5.9°), indicating that the draped field preferentially points radially downward toward the planet rather than upward.

Periodicity in the azimuth angle on a two year time scale is evident in Fig. 2a. This periodicity results because the solar zenith angle range within the 50°–60° N latitude range changes with martian season, as discussed in Section 2. Therefore, our definition of azimuth direction varies by as much as 50° in a coordinate system tied to the Sun, such as Mars solar orbital (MSO) coordinates. MSO coordinates are defined with $+\hat{x}$ toward the Sun in Mars' orbital plane, $+\hat{y}$ anti-parallel to Mars' instantaneous velocity, and $+\hat{z}$ completing the right-handed system. Indeed, the figure shows variation of roughly 50° in azimuth angle with a period of one martian year.

A second feature evident in Fig. 2 is variation in azimuth angle with a period of a month or less. This periodicity is especially strong in late 2002 and early 2003. Fig. 3 shows that the variation is strongest at periods ranging from 24.5–27 days. This period brackets the average synodic solar rotation period at Mars of 26.35 days. Fig. 3 also shows a smaller amount of power at half the sidereal solar rotation period of just over 13 days. It is likely that this trend results from passage of Mars through the different sectors of the solar wind. As the polarity of the MSO $\hat{x}$ component of the upstream IMF alternates between solar wind sectors, the polarity of the draped field at 400 km altitudes at Mars can also be expected to alternate. The alternating polarity on time scales of ∼13 days corresponds to changes of 180° in azimuth direction.

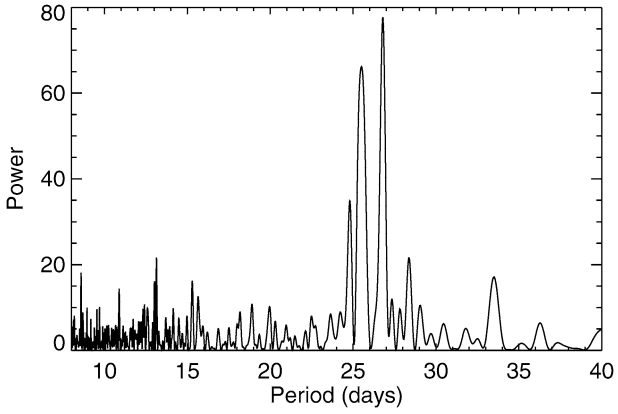

Fig. 3. Periodogram of azimuth draping direction for the orbits shown in Fig. 2. Power is shown as a function of period.

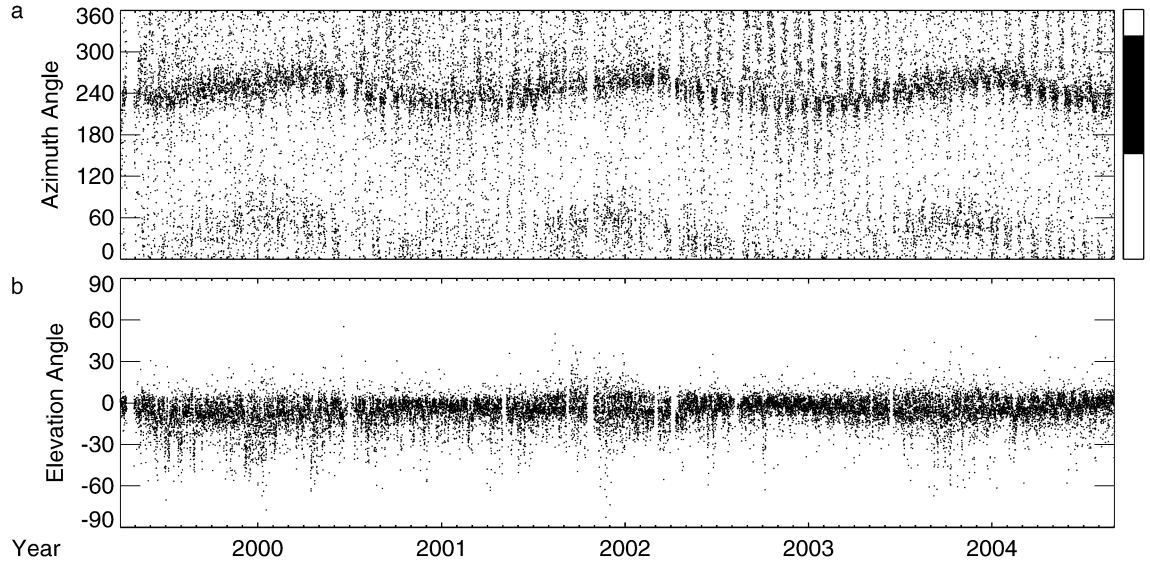

Fig. 2. Time series of draping direction inferred from day side MGS MAG data between 50 and 60° N on an orbit by orbit basis. (a) The median azimuth angle of the horizontal component of magnetic field, defined in Fig. 1. Azimuth angles of 150°–330° (the clustered draping direction referred to in Section 4) are denoted by the shaded portion of the vertical colorbar. (b) Elevation angle for each of the 22,088 orbits.

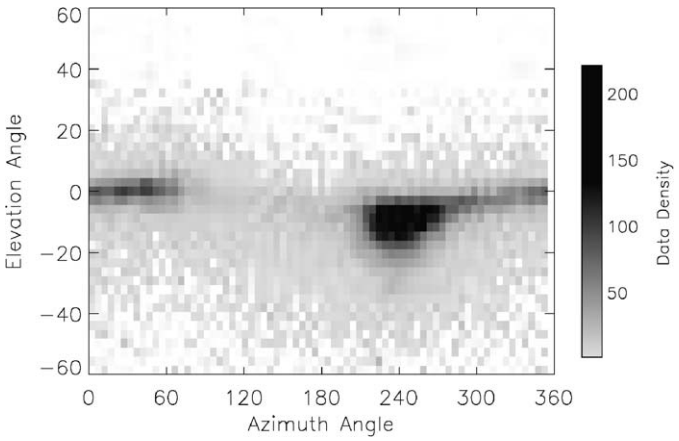

Fig. 4. Distribution of elevation angle as a function of azimuth angle for the MGS orbits shown in Fig. 2, shaded according to data density in each 5° × 3° bin.

The most striking feature evident in Fig. 2a is the non-uniform distribution of draping directions over the entire mapping phase of the MGS mission. Azimuth angles within 40° of 240° (depending upon season) are strongly preferred. That is, the magnetic field at 2 pm at 50°–60° N points locally southwest or south (roughly toward the subsolar point) much more often than it points in other directions. A second, less pronounced clustering is seen for azimuth angles near 0°–60°. Azimuth angles from 150°–330° comprise 69% of the data set in Fig. 2, so that this draping direction occurs more than twice as often as its complement.

An examination of the correlation between azimuth and elevation angle reveals that the draped field has a negative radial component during orbits when the azimuth angle is near 240° (Fig. 4). The negative median elevation angle of −5.9° discussed above simply results from the fact that many more orbits have azimuth angle near 240°. Previous investigators have shown that the draped magnetic fields are flared, so that they traverse higher altitudes near the martian terminator than at the subsolar point (e.g., Crider et al., 2004). Therefore, for orbits where the draped field at high latitudes points toward the subsolar point we would expect a negative radial field component, as observed. However, Fig. 4 does not show the expected trend that elevation angle is positive when the draped field points away from the subsolar point (near 60°). This difference might be explained if the external magnetic fields are asymmetrically draped according to the IMF direction.

A closer look at a subset of the observations from Fig. 2a (Fig. 5, top panel) reveals that the draping direction is more strongly clustered when Mars is in one solar wind sector. The favored sector for this behavior occurs when the upstream IMF is oriented such that the draped field in our sample region has azimuth angle 60°–240° (northwest), and not 240°–60° (southeast). The clustering occurs toward one edge of the possible draping directions for that sector, rather than in the middle.

What causes the difference between the distributions of draping directions in the two sectors? Is there an asymmetry in the upstream IMF orientations during this time period that propagates into the draped magnetic field on the martian day side?

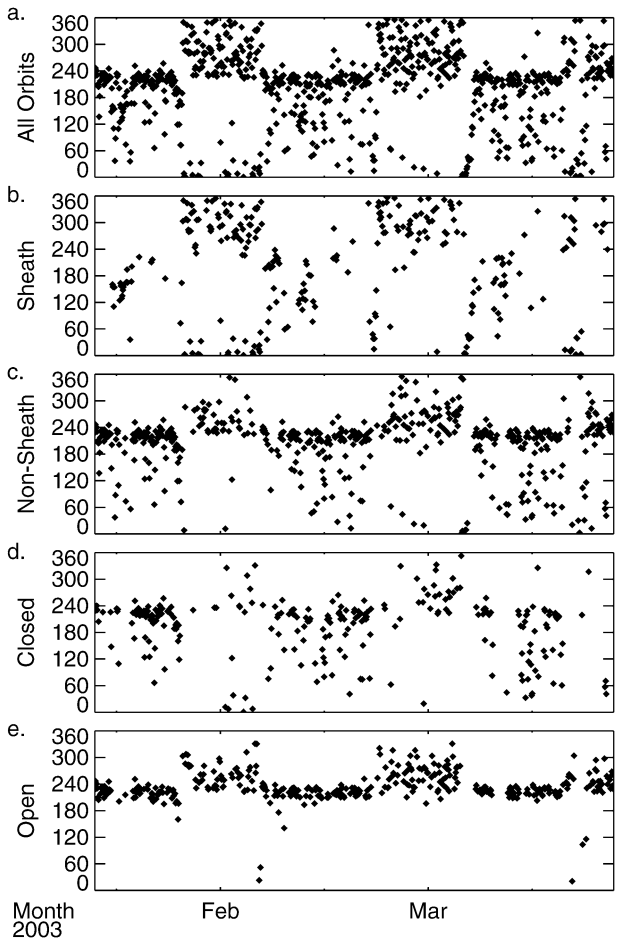

Fig. 5. Azimuth angles for a subset of orbits from Fig. 2. (a) Azimuth angles for all orbits for 70 days starting on January 1, 2003. The following panels, show: (b) only orbits when MGS sampled the sheath; (c) all non-sheath orbits; (d) orbits with closed field lines; and (e) orbits with open field lines. Criteria for selection of sheath, non-sheath, open, and closed are discussed in Section 3.

This seems unlikely, since our observations were made over a period of five years and many solar rotations. Fig. 6 shows the IMF orientation upstream of Earth's bow shock, measured by the Wind spacecraft (Lepping et al., 1995). IMF orientation is defined in this figure in geocentric solar ecliptic (GSE) coordinates. Fig. 6a shows the clock angle, or direction of the component of IMF perpendicular to the Earth–Sun line, with 0° toward $+\hat{y}$, and 90° toward $+\hat{z}$. Fig. 6b shows the spiral angle of the component of IMF parallel to the ecliptic plane, with 0° toward $+\hat{x}$, and 90° toward $+\hat{y}$. The IMF direction at Earth has periodicity on the solar rotation time scale, as at Mars. However, IMF direction is distributed similarly within each solar wind sector. There is no pronounced clustering of field directions, as there is at Mars, though the IMF is more frequently oriented toward the middle of the range of possible spiral angles in a given sector (in the preferred Parker spiral direction). We conclude that the differences between draping direction distributions observed at Mars are not propagated into the solar wind interaction region from upstream of the martian shock.

It is possible that martian crustal magnetic fields directly bias MAG measurements in our sample region on the mar-

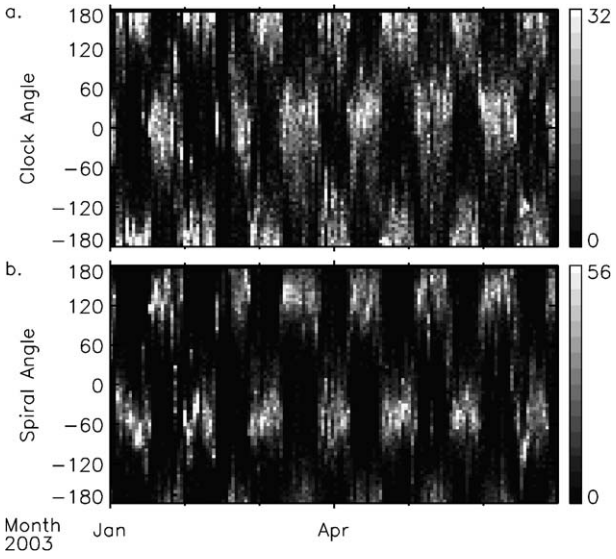

Fig. 6. Upstream IMF orientation near 1 AU as measured by the Wind MFI instrument over a period of 180 days in 2003 when Wind was well upstream of Earth's bow shock. Clock and spiral angles are measured in GSE coordinates, and are defined in the text. We used magnetometer data with a time resolution of 92 s. The figure is shaded according to data density for 1 day × 3° bins.

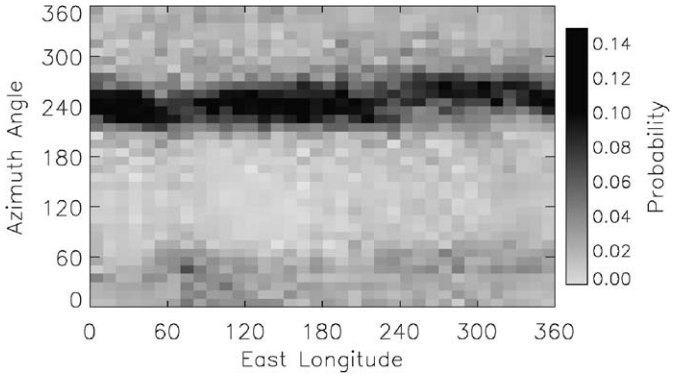

Fig. 7. Azimuth direction of the draped magnetic field at Mars as a function of the geographic longitude over which it was derived. The figure is shaded according to data density for 5° × 5° bins.

tian day side, so that our determination of draping direction is longitude-dependent. However, Fig. 7 shows that the asymmetry in azimuth direction appears to be uniformly distributed in longitude. A strong peak near 240° is seen in the figure, independent of planetary longitude. There is some indication that azimuth angles from 210°–240° are less common near 300° E than elsewhere, but the distribution is still peaked near 260° at this longitude. We conclude that crustal magnetic fields do not directly bias our determination of draping direction.

If the asymmetric distribution that we observe does not occur in the unperturbed solar wind, and is not a direct result of crustal magnetic fields contaminating our azimuth angle estimates, then it must be attributable to the physics of the martian solar wind interaction. We can help to identify the relevant physics by determining in which plasma regimes the asymmetry is observed.

As discussed in Section 2, we determine whether MGS was in or above the MPB by searching for electron energy spectra characteristic of the sheath. Fig. 5b shows the subset of orbits from the panel a for which at least one electron energy spectrum (out of typically eight or nine) from 50°–60° N was sheath-like, while panel c shows the subset of orbits for which none of the electron energy spectra was sheath-like. Our threshold for panel b was set low deliberately so that sufficient orbits were selected to identify a trend. This threshold is equivalent to selecting all orbits that pass above the bottom of the MPB. Draping directions are uniformly distributed throughout each sector for sheath-like orbits. The draping directions for non-sheath orbits, however, are more representative of the entire data set shown in panel a. Therefore, the clustering of draping directions occurs below the MPB.

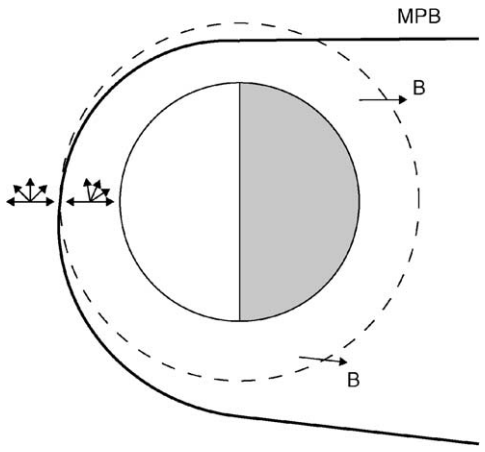

Fig. 8. Cartoon of the possible effect of an asymmetric MPB on observations of draping direction. The MGS mapping orbit is shown as a dashed line. When MGS is above the MPB the draping directions are uniformly distributed, and when it is below the MPB the draping directions are clustered. The figure is not drawn to scale. Example magnetic field vectors are shown on the nightside having the same magnitude but different radial field components.

Figs. 5b and 5c also show that MGS was above the MPB more often when the draping direction was 240°–60° than for the other IMF sector. This observation indicates that the shape of the MPB is controlled (at least in part) by the direction of the IMF. An asymmetry in the shape of the MPB has been predicted by a number of investigators (Brecht and Ferrante, 1991; Brecht et al., 1993; Harnett and Winglee, 2003). Previously, Brain et al. (2005) demonstrated that the MPB shape does vary with draping direction, though it is unclear from their analysis whether the MPB is asymmetrically shaped or changes size as the draping direction changes. A series of papers by Bertucci et al. (2003, 2004, 2005) has shown that there is a sharp change in the draping configuration of the IMF at the MPB. Therefore, when MGS is above the MPB one would expect to observe a different draping configuration then at other times, as illustrated in the cartoon in Fig. 8. If the MPB was more likely to be below MGS for one set of IMF orientations due to an asymmetric shape, then the draping directions in Figs. 2 and 5 would have different distributions for the different IMF sectors, as we observe.

Figs. 5c and 5d suggest a relationship between the clustering of draping directions and magnetic field topology. Panel d shows the subset of orbits in this time period for which at least

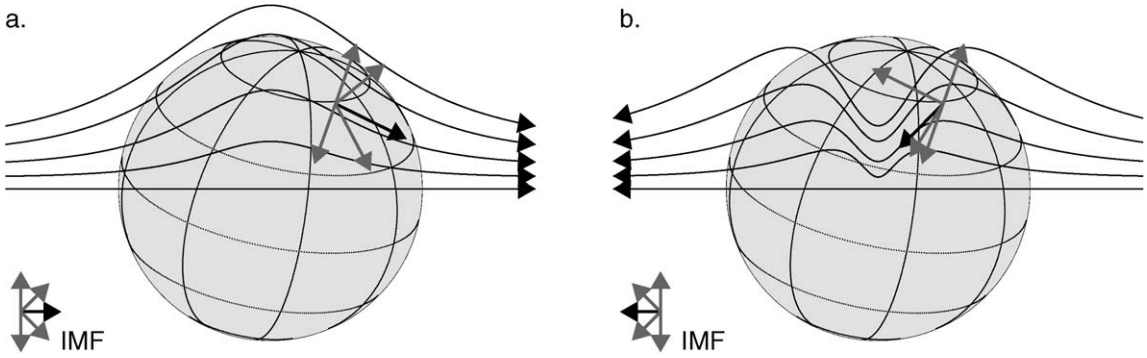

Fig. 9. Cartoon of the draping configuration close to Mars for two different orientations of the upstream field. (a) Upstream IMF oriented toward the dusk side of Mars results in a unform distribution of draping directions measured at 50°–60° N. (b) Upstream IMF oriented toward the dawn side of Mars results in a non-uniform distribution of draping directions, clustered toward ∼240°.

one electron energy spectrum has strong photoelectron signatures, which are most readily observed in the absence of solar wind electrons. Therefore, MGS likely passed through closed field regions for these orbits. Fewer closed field lines are observed when the IMF has draping direction of 240°–60° simply because MGS is in the sheath more often in this sector, and therefore "higher" in the solar wind interaction. The distribution of draping directions for orbits with closed field lines appears to be uniformly drawn from the parent population in panel a. However, when we select only orbits for which 50% or more of the electron pitch angle distributions are characteristic of open field lines we find that virtually all of the selected orbits fall within a narrow range of draping direction—especially for the 60°–240° sector. From these two panels we conclude that the clustering of draping directions occurs primarily on open field lines. Since we can only determine topology with respect to the absorption altitude for electrons in the martian ionosphere, we cannot say with certainty that the open field lines are connected to the martian crust under the present analysis. Regardless, the observations of Figs. 5 and 4 are consistent with magnetic field lines below the MPB intersecting the ionosphere at low altitudes more often when Mars is in one sector of the solar wind.

A variety of different explanations may be responsible for the observed asymmetry in draping direction. One possibility supported by the bulk of observations presented in this work is that "weathervaning" of external magnetic field lines encountering the ionosphere is more prevalent for one set of IMF orientations. Weathervaning refers to rotations in the low altitude portions of the draped magnetic field toward the anti-solar direction, in the direction of day to night ionospheric flow. This effect was studied extensively at Venus (Law and Cloutier, 1995) and reported at Mars (Cloutier et al., 1999), and results in a magnetic field configuration similar to that shown in Fig. 9b for westward IMF. This configuration is consistent with a preferred magnetic field direction in the subsolar direction at the MGS location, with negative elevation angle and evidence for electron absorption. Deviations in the upstream IMF of several degrees from westward will result in a draping direction that is generally subsolar, which could explain the observed clustering. For eastward IMF, the configuration may be more similar to the one shown in Fig. 9a, so that weathervaning either does not occur as often, or its effects are not observed at the MGS location. In this case, deviations in the upstream IMF from Eastward should result in corresponding deviations in the measured draping direction, and no clustering should be observed.

Asymmetric penetration of the IMF into the ionosphere is not the only possible explanation for the observations, nor is it complete. The MPB appears to provide an upper bound for the asymmetry. IMF-controlled hemispheric differences in charged particle motion are predicted below the MPB, both related to mass loading by planetary ions (Harnett and Winglee, 2003) and to changes in solar wind ion motion at the MPB (Brecht and Ferrante, 1991). Perhaps one of these effects provides an alternative explanation, or creates current layers that result in weathervaning. Crustal magnetic fields are also an important part of the magnetic environment below the MPB, and even locally push the MPB upward (Crider et al., 2003, 2002; Brain et al., 2003). They may also play a role in creating the observed asymmetry, perhaps through reconnection of crustal fields with the shocked IMF or through creation of ionospheric current layers that preferentially exclude the solar wind for certain IMF orientations.

4. Influence of draping direction on the global interaction

As we showed in Section 3, the magnetic field draping direction in a narrow latitude band in the northern hemisphere is asymmetrically distributed. But how does the draping direction in turn affect the more global solar wind interaction at Mars? Below we choose two features of the interaction in order to further explore the influence that IMF orientation has on Mars' magnetic environment.

4.1. Access of sheath plasma to 400 km

Access of sheath plasma to the MGS mapping altitude near 400 km has been previously studied by Brain et al. (2005), who found that the position of the MPB varies with geographic location, L_S, upstream pressure, and draping direction. Here we add to this study by examining in detail how draping direction affects the access of sheath plasma as a function of geographic location.

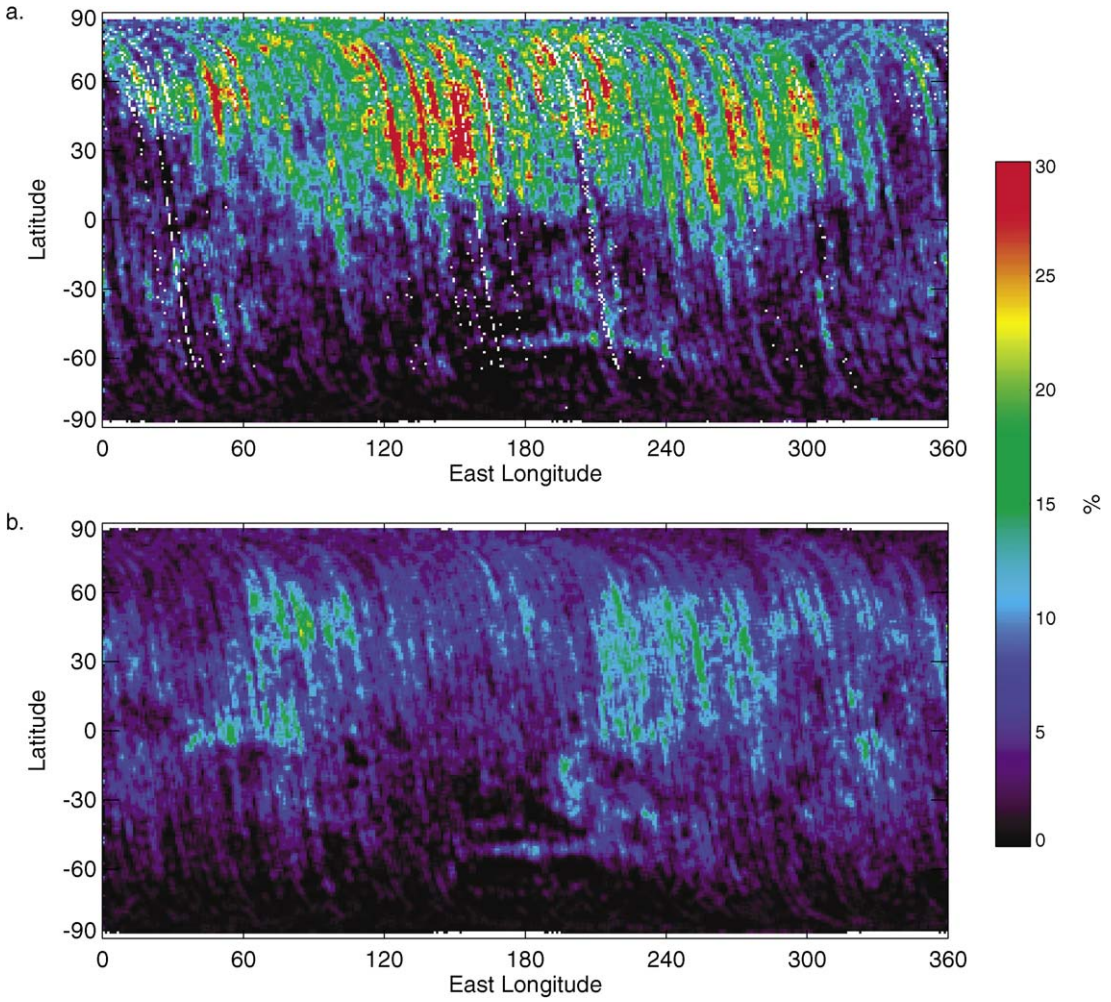

Fig. 10. Likelihood of observing sheath plasma at 2 pm as a function of geographic location for (a) draping directions from 150°–330° (the clustered direction); and (b) draping directions from 330°–150° (the unclustered direction). Day side ER energy spectra were binned as a function of longitude, latitude, and draping direction. The maps are colored according to the fraction of spectra in each bin characteristic of the sheath, then were smoothed using a 3° boxcar filter. Geographic bins are 1° × 1°.

All day side electron energy spectra in our five year time period were classified according to whether they were sheath-like (observed when MGS is above the MPB), and separated into orbits that have draping direction close to the clustered direction shown in Fig. 2 (150°–330°) and those that do not (330°–150°). For each draping direction the data were binned according to longitude and latitude. The results in Fig. 10 show the likelihood of observing sheath plasma as a function of geographic location and draping direction. There are fewer orbits with an unclustered draping direction, so panel a of has a higher noise level than panel b.

Several features are evident in both panels of Fig. 10, and have been discussed in Brain et al. (2005). Sheath plasma is excluded more often above strong crustal sources than for surrounding regions. Mini-magnetospheric cusps are evident in several locations—most notably a linear feature near 50° S stretching from 150° to 240° E, and a more compact feature centered near 200° E, 15° S. Several locations in the southern hemisphere lack strong crustal magnetic fields, yet are still less likely to have sheath plasma than similar regions in the north. This effect likely results from the slightly lower altitude of the MGS orbit when it is in the southern hemisphere.

We find three main differences between the two panels in Fig. 10. First, sheath plasma is much more likely to be observed, especially in the northern hemisphere, in the unclustered draping direction. This is simply a restatement of the results of Section 3, since clustering occurs below the MPB. If the clustered draping direction corresponds to westward upstream IMF then the global trend of Fig. 10 is also consistent with an asymmetrically shaped MPB that is lower in the mass-loaded hemisphere. The sense of this asymmetry was predicted by Brecht and Ferrante (1991).

Second, Fig. 10b shows for clustered draping directions that sheath plasma is less likely to be observed north of the strong southern crustal sources than at many other northern hemisphere locations. The opposite is true for the unclustered draping directions. It appears that crustal magnetic fields, either in the southern hemisphere or some other nearby location such as the crustal source near the North Pole, influence the access of sheath plasma to 400 km from distances of hundreds or thousands of kilometers.

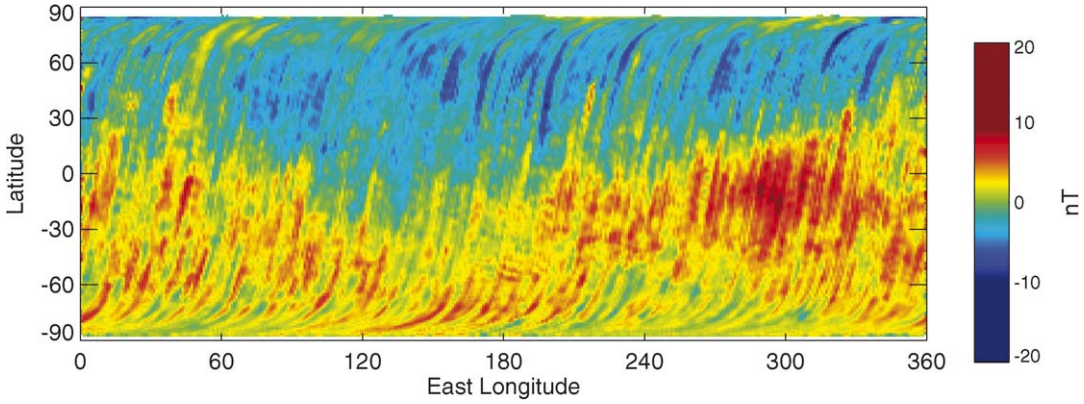

Fig. 11. The difference in the average radial magnetic field at 2 am on the night side of Mars for two different draping azimuth angles, as a function of longitude and latitude. The radial magnetic field component for all MAG observations made in the planet's optical shadow were classified according to the draping azimuth for each orbit, as in Fig. 10. The median radial field component was computed for each $1^\circ \times 1^\circ$ geographic bin. The map above is colored according to the difference between the map for 330°–150° azimuth angles and the map for 150°–330° azimuth angles.

Third, some regions of weak crustal magnetic field appear to behave oppositely for the two draping directions. For example, note the weak sources centered near (80° E, 35° N), (55° E, 0° N), and (330° E, 10° S). In these regions, sheath plasma is more commonly observed for the clustered draping direction, opposite the global trend. The draping direction affects the local access of sheath plasma near crustal magnetic fields.

One interpretation for these last two trends is that reconnection of crustal magnetic fields to the shocked IMF proceeds more readily for the clustered orientation, so that sheath electrons are able to access 400 km altitudes in mini-magnetospheric cusps. One can imagine magnetic field lines from the sheath connected to cusps for one IMF orientation, and draped over them for the other. This idea is consistent with the result from Section 3 that the clustered magnetic field direction is associated with open field lines.

4.2. Night side vertical magnetic fields

The optical shadow is an important region of the martian solar wind interaction. It contains the night side plasma sheet (Dubinin et al., 1991; Ferguson et al., 2005), a steady outflow of escaping oxygen ions (Kallio et al., 1995), and is the region used as the primary source of information about unperturbed crustal magnetic fields, since external fields are weaker and the plasma environment is less turbulent than the day side (Connerney et al., 2001). While external fields are nearly entirely horizontal on the day side of Mars, the radial field component comprises a larger fraction of the total field on the night side in MGS data (Brain et al., 2003). Here we examine whether and how the day side draping direction affects the radial component of the night side field.

Magnetic field observations in the optical shadow of Mars over our five year time period were separated by orbit according to their draping direction (clustered or unclustered). The mean radial magnetic field component was computed as a function of longitude and latitude for each draping direction, and the unclustered map was subtracted from the clustered map. The difference between the average radial magnetic field for the two draping directions is shown in Fig. 11. This difference can be as high as 10–15 nT in some geographic locations, and is organized mostly by latitude.

One potential explanation for this asymmetry is related to the flare angle of the draped field, controlled by E_{SW}. On the day side, such an asymmetry would create hemispheric differences in the radial magnetic field component for a given IMF orientation, since the draped external field would be more inclined in one hemisphere. This difference would translate to the night side as well (see Fig. 8). When the average radial field configuration for unclustered draping directions is subtracted from that for clustered draping directions, we are in fact subtracting two patterns with a hemispheric asymmetry. The end result is shown in Fig. 11.

One troubling aspect of this explanation, however, is that there is no reason to expect the differences in radial field to depend upon planetary longitude. Fig. 11 shows a sinusoid in the polarity of the difference near the equatorial plane of Mars. The "North Pole" of this sinusoid is located near 150° E and 50° N. This feature suggests that some effect tied to the planet itself may be at least partly responsible for the observed difference in radial field. Looking at Fig. 11, however, crustal magnetic fields do not appear to play a large role in this difference since they cannot be distinguished in the figure.

5. Summary

This paper explores the relationship between the orientation of draped magnetic fields at Mars and the global solar wind interaction. Using statistical methods, we discovered three trends in the draping direction. A periodicity on the time scale of a martian year is explained by the annual "wobbling" back and forth of the MGS orbit in MSO coordinates. Periodicity on 26 day time scales is explained by the passage of different IMF sectors (having different magnetic field polarities) past Mars. And an asymmetry in the distribution of draping directions is observed only when MGS is below the MPB (which is most of the time). This asymmetry is created by a clustering of draping directions when Mars is in one IMF sector, and a more

uniform distribution when it is in the other IMF sector. This trend is consistent with rotation in the anti-solar direction of draped field lines that preferentially penetrate into the deep ionosphere for one set of upstream IMF orientations. Effects that may cause this asymmetric weathervaning (or instead may explain the observations on their own) include asymmetric solar wind ion motion, mass loading, magnetic reconnection of the IMF to crustal magnetic fields, or current layers near crustal magnetic fields.

We showed in Section 4 that the draped field orientation also affects the global solar wind interaction. Sheath plasma has more frequent access to certain geographic locations depending upon the draping direction. Crustal magnetic fields appear to affect the differences in this access on both large and small spatial scales. The average radial magnetic field component on the night side can be different by 10–15 nT in some locations depending upon the draping direction. This difference probably results from an asymmetry in the flaring angle of the draped field on the day side.

Many questions are left unexplained by this work. We have not identified the root cause of the draping asymmetry. We have not explored how crustal fields influence the access of sheath plasma, but suspect that magnetic reconnection plays a role. And we have not explained why the observed difference in average radial field with draping direction depends upon planetary longitude.

At present a few possible avenues may provide the information necessary to answer these questions. First, continued study of the MGS data set is a necessity, specifically in the area of magnetic field topology. However, MGS is now in an orbit that samples a limited portion of the solar wind interaction region at Mars (albeit repeatedly). Continued modeling efforts will give a more global picture of how IMF orientation affects the solar wind interaction. And information from the ASPERA-3 experiment on Mars Express will prove extremely useful for two reasons. First, the Mars Express orbit covers more of the parameter space in local time and altitude of the interaction region. Second, Mars Express provides simultaneous measurements (including ions) with MGS MAG/ER.

Acknowledgments

D. Brain acknowledges useful discussions with J. Luhmann and D. Crider. This work was supported under NASA Grant NNG04GL35G-05/06.

References

Acuña, M.H., and 12 colleagues, 2001. The magnetic field of Mars: Summary of results from the aerobraking and mapping orbits. J. Geophys. Res. 106 (E10), 23403–23418.

Bertucci, C., Mazelle, C., Acuña, M.H., Russell, C.T., Slavin, J.A., 2003. Magnetic field draping enhancement at the martian magnetic pileup boundary from Mars global surveyor observations. Geophys. Res. Lett. 30 (2), doi:10.1029/2002GL015713. 1099.

Bertucci, C., Mazelle, C., Crider, D.H., Mitchell, D.L., Sauer, K., Acuña, M.H., Connerney, J.E.P., Lin, R.P., Ness, N.F., Winterhalter, D., 2004. MGS MAG/ER observations at the magnetic pileup boundary of Mars: Draping enhancement and low frequency waves. Adv. Space Res. 33, 1938–1944, doi:10.1016/j.asr.2003.04.054.

Bertucci, C., Mazelle, C., Acuña, M.H., Russell, C.T., Slavin, J.A., 2005. Structure of the magnetic pileup boundary at Mars and Venus. J. Geophys. Res. 110, doi:10.1029/2004JA010592. A01209.

Brain, D.A., 2002. The influence of crustal magnetic sources on the topology of the martian magnetic environment, Ph.D. thesis, University of Colorado.

Brain, D.A., Bagenal, F., Acuña, M.H., Connerney, J.E.P., 2003. Martian magnetic morphology: Contributions from the solar wind and crust. J. Geophys. Res. 108 (A12), doi:10.1029/2002JA009482. 1424.

Brain, D.A., Mitchell, D.L., Lillis, R., Lin, R., 2004a. Observations of open and closed magnetic field lines at Mars: Implications for the upper atmosphere. In: AAS/DPS Meeting Abstracts, vol. 36. Abstract 37.19.

Brain, D.A., Mitchell, D.L., Lillis, R., Lin, R., 2004b. Use of martian magnetic field topology as an indicator of the influence of crustal sources on atmospheric loss. In: AGU Fall Meeting Abstracts. Abstract SA13A–1119.

Brain, D.A., Halekas, J.S., Lillis, R.J., Mitchell, D.L., Lin, R.P., Crider, D.H., 2005. Variability of the altitude of the martian sheath. Geophys. Res. Lett. 32 (18), doi:10.1029/2005GL023126. L18203.

Brecht, S.H., Ferrante, J.R., 1991. Global hybrid simulation of unmagnetized planets: Comparison of Venus and Mars. J. Geophys. Res. 96 (A7), 11209–11220.

Brecht, S.H., Ferrante, J.R., Luhmann, J.G., 1993. Three-dimensional simulations of the solar wind interaction with Mars. J. Geophys. Res. 98 (A2), 1345–1357.

Cloutier, P.A., and 19 colleagues, 1999. Venus-like interaction of the solar wind with Mars. Geophys. Res. Lett. 26 (17), 2685–2688.

Cloutier, P.A., McElroy, M.B., Michel, F., 1969. Modification of the martian ionosphere by the solar wind. J. Geophys. Res. 74 (26), 6215–6228.

Connerney, J.E.P., Acuña, M.H., Wasilewski, P.J., Kletetschka, G., Ness, N.F., Rème, H., Lin, R.P., Mitchell, D.L., 2001. The global magnetic field of Mars and implications for crustal evolution. Geophys. Res. Lett. 28 (21), 4015–4018.

Crider, D., 2004. The influence of crustal magnetism on the solar wind interaction with Mars: Recent observations. Adv. Space Res. 33, 152–160, doi:10.1016/j.asr.2003.04.013.

Crider, D., and 18 colleagues, 2000. Evidence of electron impact ionization in the magnetic pileup boundary of Mars. Geophys. Res. Lett. 27 (1), 45–48.

Crider, D.H., Vignes, D., Krymskii, A.M., Breus, T.K., Ness, N.F., Mitchell, D.L., Slavin, J.A., Acuña, M., 2003. A proxy for determining solar wind pressure at Mars using Mars Global Surveyor data. J. Geophys. Res. 108 (A12), doi:10.1029/2003JA009875. 1461.

Crider, D.H., and 12 colleagues, 2002. Observations of the latitude dependence of the location of the martian magnetic pileup boundary. Geophys. Res. Lett. 29. 11-1.

Crider, D., Brain, D.A., Acuña, M., Vignes, D., Mazelle, C., Bertucci, C., 2004. Mars Global Surveyor observations of solar wind magnetic field draping around Mars. Space Sci. Rev. 111, 203–221.

Dubinin, E., Lundin, R., Riedler, W., Schwingenschuh, K., Luhmann, J.G., Russell, C.T., Brace, L.H., 1991. Comparison of observed plasma and magnetic field structures in the wakes of Mars and Venus. J. Geophys. Res. 96 (A7), 11189–11197.

Dubinin, E., Sauer, K., Delva, M., Tanaka, T., 1998. The IMF control of the martian bow shock and plasma flow in the magnetosheath: Predictions of 3-D simulations and observations. Earth Planets Space 50, 873–882.

Dungey, J.W., 1961. Interplanetary magnetic field and auroral zones. Phys. Rev. Lett. 6 (2), 47.

Ferguson, B., Cain, J.C., Crider, D.H., Harnett, E., Brain, D.A., 2005. External fields on the night-side of Mars at Mars Global Surveyor mapping altitudes. Geophys. Res. Lett. 32, doi:10.1029/2004GL021964. L16105.

Harnett, E.M., Winglee, R.M., 2003. The influence of a mini-magnetopause on the magnetic pileup boundary at Mars. Geophys. Res. Lett. 30 (20), doi:10.1029/2003GL017852. 2074.

Kallio, E., Koskinen, H., Barabash, S., Nairn, C., Schwingenschuh, K., 1995. Oxygen outflow in the martian magnetotail. Geophys. Res. Lett. 22 (18), 2449–2452.

Law, C.C., Cloutier, P.A., 1995. Observations of magnetic structure at the dayside ionopause of Venus. J. Geophys. Res. 100 (A12), 23973–23981.

Lepping, R.P., and 14 colleagues, 1995. The wind magnetic field investigation. In: Russell, C.T. (Ed.), The Global Geospace Mission. Kluwer Academic, Dordrecht, pp. 207–229.

Mitchell, D.L., Lin, R.P., Mazelle, C., Rème, H., Cloutier, P.A., Connerney, J.E.P., Acuña, M.H., Ness, N.F., 2001. Probing Mars' crustal magnetic field and ionosphere with the MGS Electron Reflectometer. J. Geophys. Res. 106 (E10), 23419–23427.

Nagy, A.F., and 14 colleagues, 2004. The plasma environment of Mars. Space Sci. Rev. 111 (1), 33–114, doi:10.1023/B:SPAC.0000032718.47512.92.

Øieroset, M., Mitchell, D.L., Phan, T.D., Lin, R.P., Crider, D.H., Acuña, M.H., 2004. The magnetic field pile-up and density depletion in the martian magnetosheath: A comparison with the plasma depletion layer upstream of the Earth's magnetopause. Space Sci. Rev. 111 (1), 185–202.

Paschmann, G., Sonnerup, B.U.O., Papamastorakis, I., Sckopke, N., Haerendel, G., Bame, S.J., Asbridge, J.R., Gosling, J.T., Russell, C.T., Elphic, R.C., 1979. Plasma acceleration at the Earth's magnetopause: Evidence for magnetic reconnection. Nature 282, 243–246.

Vignes, D., Acuña, M.H., Connerney, J.E.P., Crider, D.H., Rème, H., Mazelle, C., 2002. Factors controlling the location of the Bow Shock at Mars. Geophys. Res. Lett. 29 (9), doi:10.1029/2001GL014513. 1328.

Yeroshenko, Y., Riedler, W., Schwingenschuh, K., Luhmann, J.G., Ong, M., Russell, C.T., 1990. The magnetotail of Mars: Phobos observations. Geophys. Res. Lett. 17 (6), 885–888.

Zhang, T.L., Schwingenschuh, K., Lichtenegger, H., Riedler, W., Russell, J.G., Luhmann, C.T., 1991. The magnetic barrier at Venus. J. Geophys. Res. 96 (A7), 11265–11269.